Environmental Science and Pollution Research (2020) 27:45390–45404
https://doi.org/10.1007/s11356-020-10311-3

RESEARCH ARTICLE

Experimental investigation on lowering the environmental hazards and improving the performance patterns of solar flat plate collectors by employing the internal longitudinal fins and nano additives

Dinesh Babu Munuswamy [1] · Yuvarajan Devarajan [2] · M. Naresh Babu [3] · Sathiyamoorthi Ramalingam [1]

Received: 28 April 2020 / Accepted: 28 July 2020 / Published online: 13 August 2020

Abstract
The main objective of this study is to lower the greenhouse gases by developing and optimizing a solar flat plate collector. The rifled tube is integrated into the collector to increase the thermal heat transfer thereby improving its performance. Two flat plate collectors, one with in-housed longitudinal fins and another without fins of 0.5 m^2 collector area, have been intended and fabricated with provisions for K-type thermocouples to examine the temperature variations inside the collector for different working fluids. This current study reveals using CuO and Al_2O_3 nanoparticles in varying weight fractions in incremental order to study the effect of weight fractions on the efficiency of the collector. The simulation was done using computational fluid dynamics both for the finned and without finned tube collectors separately and the outcome of the results for the collector outlet temperatures is compared with the experimental one and results show a valuable outcome for the intended collectors. Initially, the test was conducted with pure distilled water as working fluid and further nanoparticles were opted and doped inside the collector side for varying weight fractions of 0.2% and 0.4% and their results are compared. The experimental results showed an improved heat transfer was pragmatic in the collector side for using nanoparticles. Mixing the nanofluids exhibited superior efficiency on the collector side. The results showed after successful trials of experimentation, doping of CuO nanoparticles by varying weight fractions of 0.2% and 0.4%, augmentation of the collector (unfinned) efficiency is 2.1% and 4.05%, and similarly for finned tube collector, it is 3.02% and 5.5% for same weight fractions. In order to improve the thermal efficiency of collector, CuO is replaced by Al_2O_3 nanoparticles; for dissimilar weight fractions, the efficiency is enhanced nearly by 3.7% and 6.54% for unfinned tube collector, and for the finned tube, the collector is 4.8% and 7.8% respectively, compared with the base working fluid (water). Experimentation of the collectors with finned tube type achieved a superior efficiency compared with that of unfinned tube collectors which is proved to be higher when used for nanofluids to that of the base working fluid water.

Keywords Greenhouse gases · Solar energy · Collectors · Efficiency · Nanoparticles

Nomenclature

Al_2O_3	Aluminium oxide
CuO	Copper oxide
MHPAC-FPC	Micro heat pipe array-flat plat collector
BN	Boron nitride
MWCNT	Multi-walled carbon nanotubes

Editorial Responsibility: Philippe Garrigues

✉ Dinesh Babu Munuswamy
dinesh198014@yahoo.com

Yuvarajan Devarajan
dryuvarajand@mits.ac.in

M. Naresh Babu
narsavi@gmail.com

Sathiyamoorthi Ramalingam
sathiya.ram78@gmail.com

[1] Department of Mechanical Engineering, Panimalar Engineering College, Poonamallee, Chennai 600123, India

[2] Department of Mechanical Engineering, Madanapalle Institute of Technology and Science, Madanapalle, Andhra Pradesh, India

[3] Department of Mechanical Engineering, GRT Institute of Engineering and Technology, Tiruttani, Tamil Nadu, India

SWCNTs	Single-wall carbon nanotubes
CNT	Carbon nanotubes
H_2O	Water
CFD	Computational fluid dynamics
TiO_2	Titanium di oxide
nm	Nanometre
Ag	Silver
OD	Outer diameter
LPD	Litres per day
SFPWHS	Solar flat plate water heating systems
FPC	Flat plate collector
SFPC	Solar flat plate collector
SEM	Scanning electronic microscope
CTAB	Cetyl methyl ammonium bromide
EDAX	Energy-dispersive X-ray analysis

Introduction

Reducing the design cost of a solar collector can be obtained using a stumpy material (reduction in durability) or by altering the geometry of the collectors. Deduction of the overall collector area can be made probable which is the best method of improving the transmission of heat rate. More methods have been employed and various experiments were conducted to perk up the thermal performance of solar water heaters. As an attempt in the direction to enhance the overall efficiency of solar collector's nano additives of CuO, it is mixed with base working fluid water by varying weight fractions and in the flat plate collector (Aruna et al. 2015). Up-gradation in the collector efficiency would lay concrete for prerequisite by reducing the size of collector area thereby decreasing the cost for solar flat plate collector (Daniels et al. 2019; Kumar 2019). Dinesh Babu and Venkata Ramanan 2016) studied experimentally by comparing three different

Fig. 2 Photograph of the experimental setup

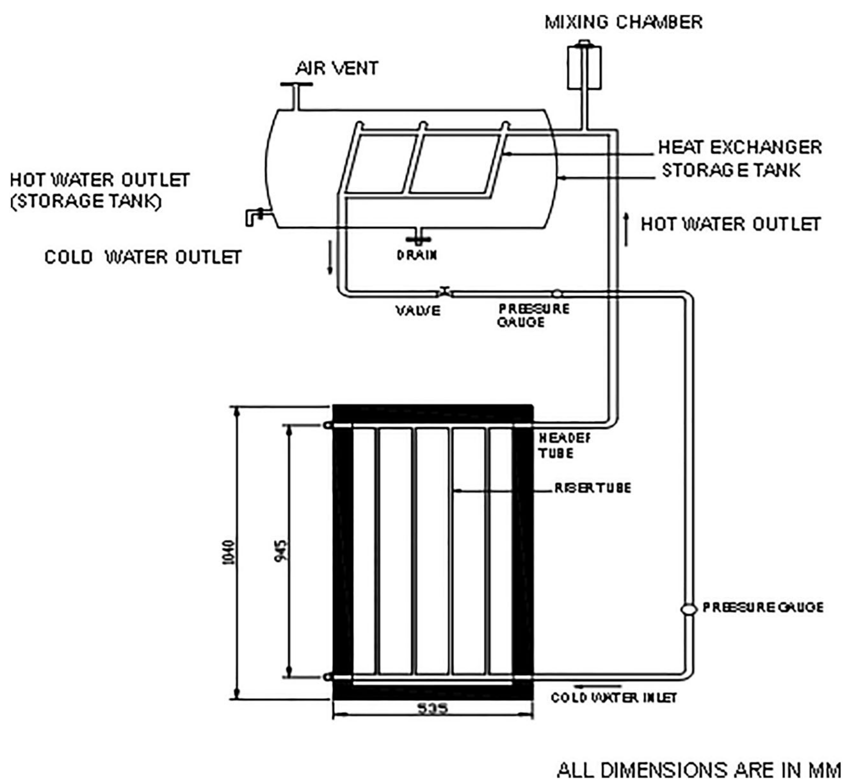

Fig. 1 Experimental setup of solar flat plate collector

Table 1 Specifications of solar flat plate collector

Parameters	Dimensions
Tank capacity	25 LPD
Length of collector (L)	945 mm
Width of the collector (w)	420 mm
Inner diameter of tube (d_i)	8.73 mm
Outer tube diameter (d_o)	9.52 mm
Pitch of the tube (t_P)	100 mm
Number of tubes (N)	4
Thermal conductivity of plate material	386 W/mk
The thickness of the collector plate	1 mm
Height of fin	20 mm
Insulation material	Glass wool

nanofluids of alumina, copper and zirconium of varying weight fractions of 0.2% and 0.4%. Results showed a maximum efficiency of 55% for 0.4% Al_2O_3 nanofluids. Huiminliu et al. (2015) studied a solar water heating system by micro heat pipe array-flat plat collector (MHPAC-FPC) in accordance with solar irradiation, and the result showed there is a substantial augmentation in collector efficiency nearly 62%. Dinesh Babu and Venkata Ramanan (2015) investigated two different solar collectors of and un-finned and finned collectors using Al_2O_3 nanofluids. Results showed for finned-tube collector efficiency is increased for 3–4% when compared with unfinned type collectors compared with base working fluid. Dinesh Babu and Venkata Ramanan (2016) configured two different collectors, one with internal fin and without a fin, and the result showed efficiency improvement of

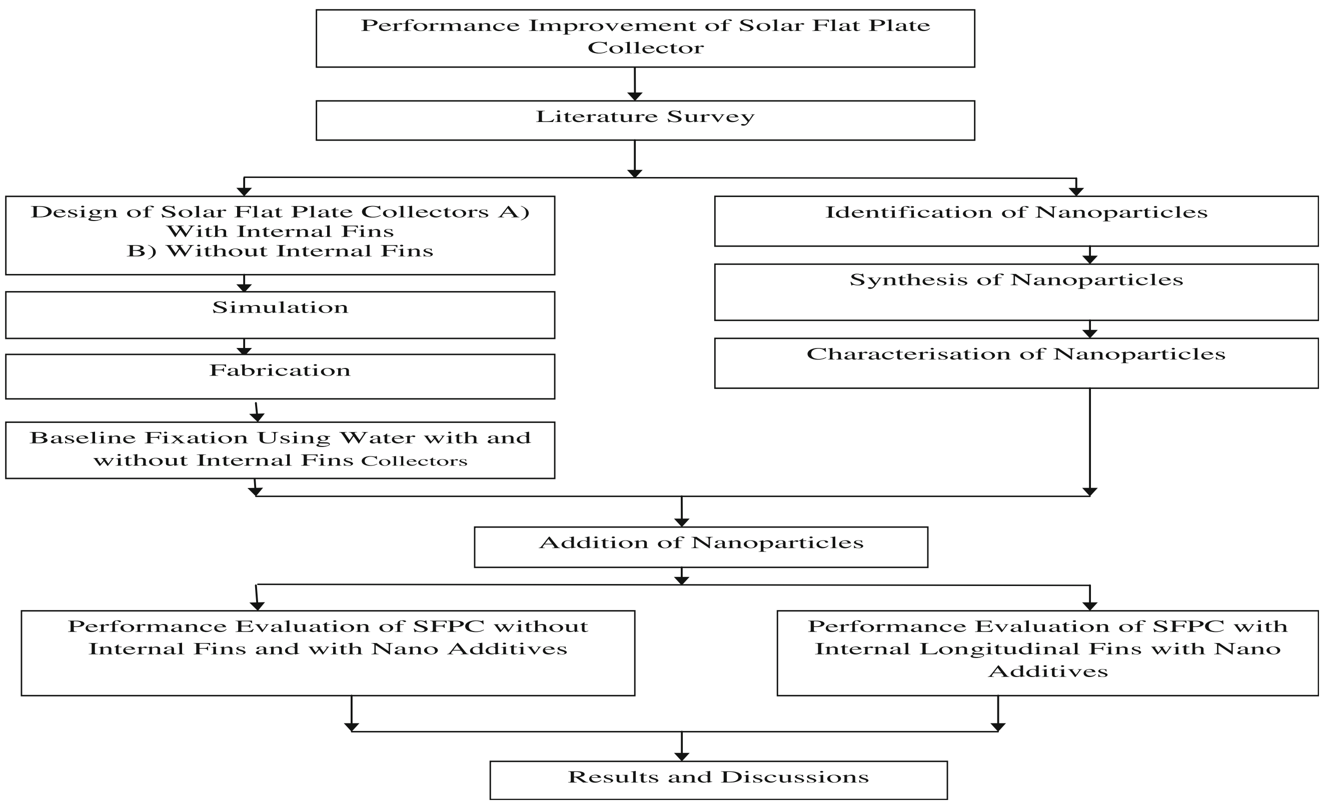

Fig. 3 Methodology flowchart

Table 2 Details of the synthesized nanoparticles

Products	Raw material	Product size (nm)	Monolayer volume (cm^3/g)	Surface area by BET method (m^2/g)	Density (kg/m^3)	Colour of salt	Colour of the product
Alumina	Aluminium nitrate	20	62.95	274.01	3960	White	Pale yellow
Copper oxide	Copper nitrate	50	2.07	9.05	6200	Blue	Dark Brown

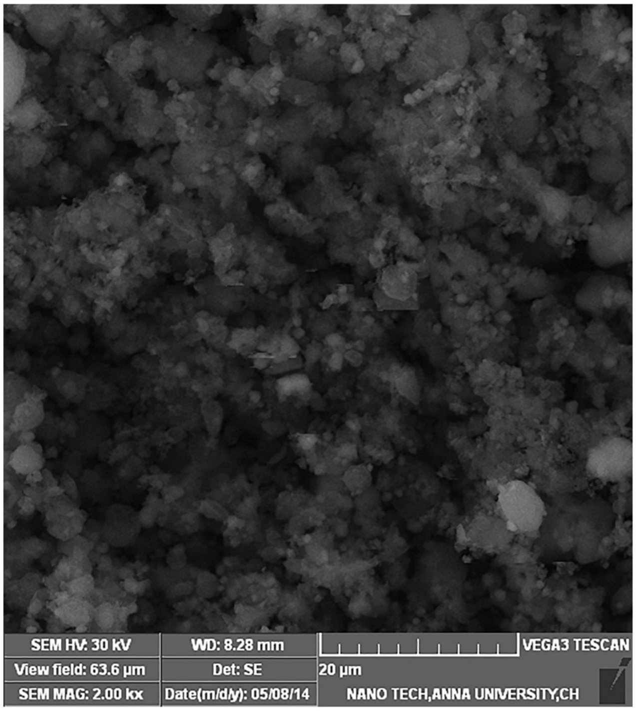

Fig. 4 SEM image of Al_2O_3

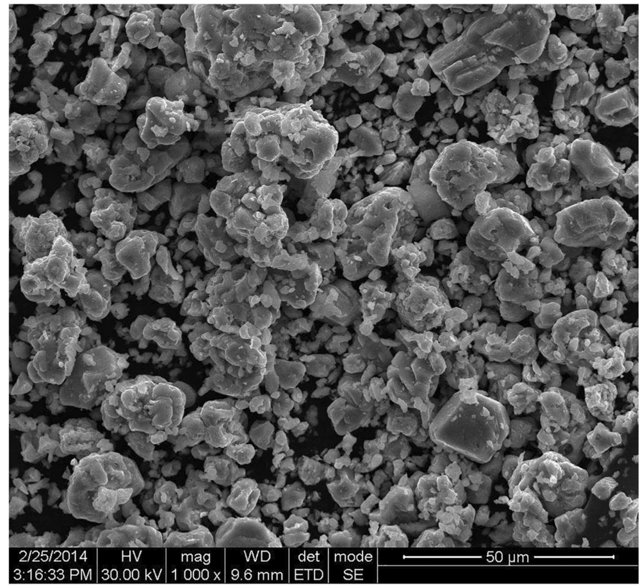

Fig. 6 SEM image of CuO

nearly 4.5% compared with that of unfinned tube collector. Shkhair and Sanke (2015) conducted a CFD analysis for helical fin and without fin riser tube solar collectors. The result showed that for the same boundary conditions during the analysis, outlet temperature is enhanced by 9.2 K and efficiency is 18.2% higher for helical fins compared with that of without fin-type solar collectors. Karmare and Tikekar (2010) analysed solar air heater using CFD for the fluid flow and heat transfer, for circular, a square and triangular cross section in a rib grit roughened surface. The results reveal that a square cross-sectional ribs with 58° leads to better heat transfer of nearly 30% for roughened plate over the smooth surface. Yousefi et al. (2012) investigated the flat plate collector of area 2.0 m^2 using the base working fluid water, as well as Al2O3/water nanofluids with a particle size of 15 nm at a weight concentration of 0.2% and 0.4%, and test was carried out using with and without surfactant TirtonX-100. The result showed efficiency was nearly 28.3% which is achieved for 0.2% weight fraction using surfactants and 15.63% achieved without surfactant with nanofluids. Yousefi and Veisy (2012) examined the effect of multi-walled carbon nanotubes (MWCNT) for weight fraction of 0.2% and 0.4% using TritonX-100 has surfactant with varying mass fraction of 0.0167–0.05 kg/s. The result showed that through an increase in the weight fractions from 0.2 to 0.4%, there is a significant augmentation

Fig. 5 EDAX of Al_2O_3

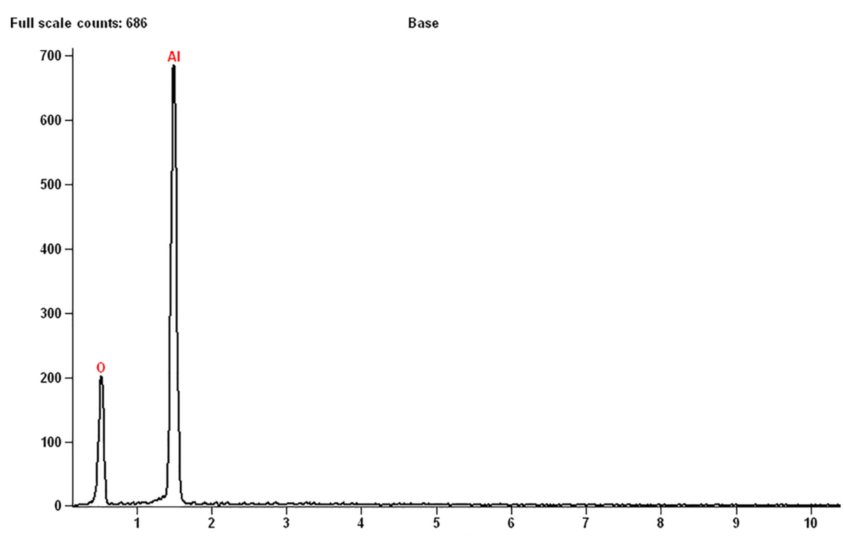

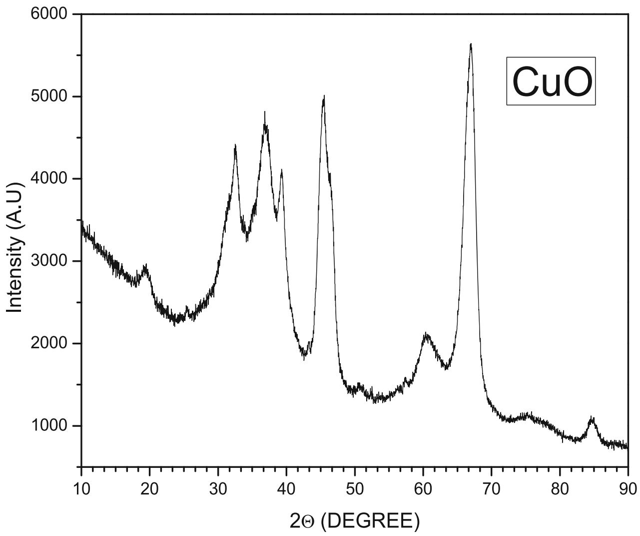

Fig. 7 EDAX of CuO

Fig. 8 Ultrasonicator

in the collector efficiency increased by 45.84 and 65.51% respectively. Said et al. (2014) establish that the use of the single-wall carbon nanotube (SWCNT) nanofluids in a flat plate solar collector shows the least entropy generation weighted against Al_2O_3, TiO_2 and SiO_2 nanoparticles in the same host fluid. Decrease in the entropy generation through 4.34% as well as the augmentation of the coefficient of heat transfer by15.33% was observed as a result of SWCNT nanofluids. Okafor (2013) conducted experiments on a designed solar water heater which works by the principle of them syphoning whose thickness is 50 mm, made up of fibreglass of collector area 1.6 m^2 at a tilted angle of 7° (degree). The result showed the attainment of an utmost temperature of 72 °C at an average gain in energy of 24 W/h and efficiency of solar water heater is 42.4%. Gangadevi et al. (2013) conducted experiments revealing that the thermal efficiency of a flat plate solar collector could be improved by increasing the nanoparticle volume fraction and selecting a nanofluid possessing higher thermal conductivity. Tiwari et al. (2013) carried out a study of a solar flat plate collector using Al_2O_3 nanofluids for volume fractions of 0.5, 1.0 and 1.5%. The result showed that the maximum efficiency of 31.64% was obtained at a volume fraction of 1.5% nanofluid. He et al. (2011) performed the test with two different working nanofluids of TiO_2/H_2O and CNT/H_2O, and the result inferred for 0.5% carbon nanotube (CNT) based water nanofluids is better opted working fluid for better light heat conversion on a vacuum tube solar collector. Faizal et al. (2013) focussed on the impacts of a decrease in the collector's size using the nanofluids as base fluids. Multi-walled carbon nanotube (MWCNT) nanofluids were used for diverse weight fractions of 0.2 and 0.4% fractions with and without surfactant and tested for its efficiency. Lu (2011) investigated the thermal performance of water-rooted CuO nanofluids in an open type thermosyphon evacuated tubular collectors. The results showed that using CuO nanofluids for the mass fraction of 1.2% in an evacuated tube collector improves the rate of heat transfer which augment the collector competence. Aparna et al.'s (2019) study observed the thermal conductivity of hybrid nanofluid Al_2O_3-Ag is almost same as of silver nanofluid, and most importantly, it was noted that hybrid nanofluid has a good stability period of time. Michael and Iniyan (2015) employed CuO/H_2O nanofluid of 0.3–0.21 nm average crystalline size and 0.05 vol% in solar collector (flat plate). The efficiency reached 52.33% by water and the efficiency further enhanced to 58% using nanofluid. Qu et al. (2019) experimented using CuO, MWCNT and CuO-MWCNT nanofluid indirect absorption solar collector and results exhibited those hybrid nanofluids (CuO-MWCNT) have maximum efficiency

Table 3 Thermal properties of synthesized nanofluids

Nanofluid	Concentration	Thermal conductivity (W/mK)	Density (kg/m^3)	Specific heat (J/kg K)
Al_2O_3	0.2%	0.6992	1178	3493
	0.4%	0.7901	1118	2983
CuO	0.2%	0.641	1208	2917
	0.4%	0.7322	1416	3423

Fig. 9 Magnetic stirrer to ensure uniform dispersion for CuO nanofluid

compared with the base fluids. Analysis of literature revealed that no significant work has been carried out on solar flat plate water heating system using internal fins and nanofluids.

Materials and methods

Design of solar water heater

The basic elements of a solar water heater are the following:

a) Storage tank
b) Flat plate collector
c) Insulators and
d) Circulation system

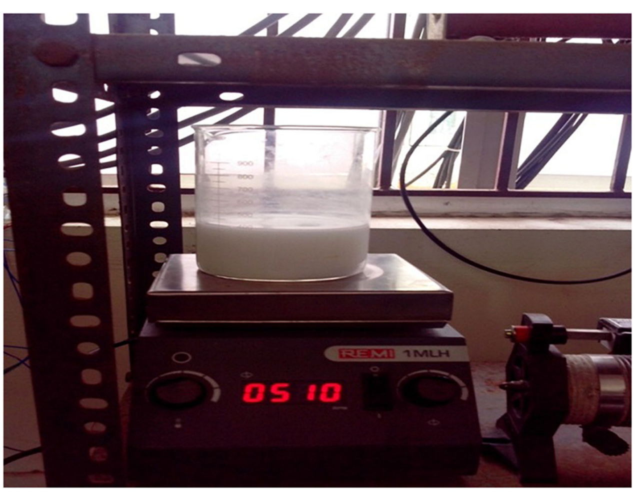

Fig. 10 Magnetic stirrer to ensure uniform dispersion for Al_2O_3 nanofluid

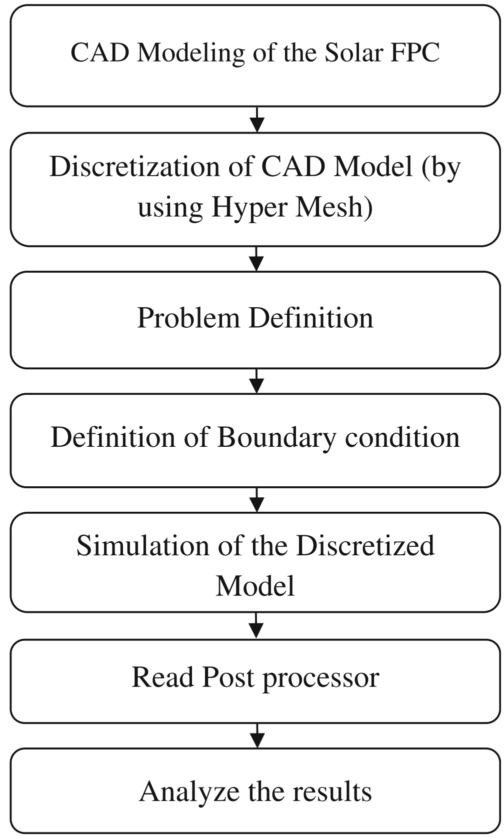

Fig. 11 Flowchart for simulation

Based on the literature survey, a 25-LPD natural circulation solar flat plate collector has been designed adopting dual circuit concept. The primary circuit forms the flat plate collector while the secondary circuit (ladder-type heat exchanger) is linked to the storage tank. The holding capacities of these circuits are 2.5 l and 25 l respectively. Dual circuit concept has been adopted for it has been planned to use nanofluids as the heat transfer fluid. The collector is designed with four parallel riser 12-mm OD copper tubes of 1000 mm in length. Headers of 25.4-mm OD have been designed for supplying/collating water from the riser tubes. The outlet of the collector has been coupled to the ladder-type heat exchanger present in the storage tank. Provisions were made in the storage tank for collecting hot water and supplying cold water. The outlet from the ladder-type heat exchanger is attached to the inlet of the

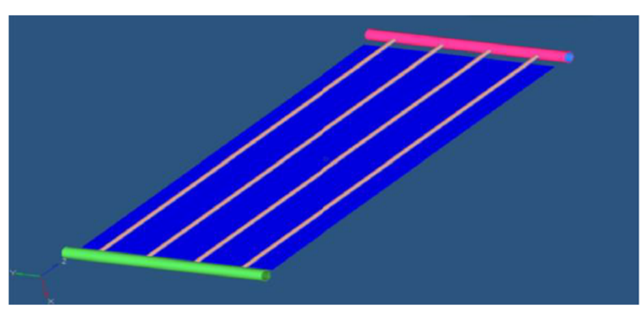

Fig. 12 Solar collector model created using Pro-E

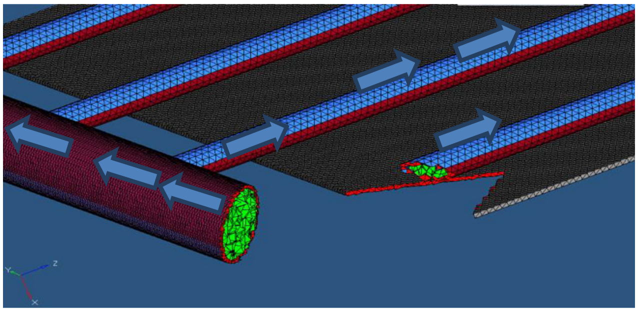

Fig. 13 Meshed model using HyperMesh

flat plate collector thereby forming a looping arrangement. Figures 1 and 2 depict the design of the experimental setup and photographic view and Table 1 details the specifications arrived at. Other general attachments like makeup water, sacrificial anode and air vent had been provided at appropriate locations.

Methodology

The objective of the study could be broadly summarized as lowering the cost of conventional solar flat plate water heating system collector by reducing the collector area, which can be attained by enhanced heat transfer (providing longitudinal internal fins and nanoparticles). Figure 3 depicts the methodology adopted for achieving the objective.

Selection, synthesis and characterisation of nanoparticles

The conventional approach of dispersing millimetre or micrometre-sized particles in liquids for enhanced heat transfer has three major technical problems, viz. rapid settling, poor thermal conductivity at lower particle concentrations and clogging of flow channels Chatur and Nitnaware 2015. Nanofluids prepared from alumina/copper oxide were selected for carrying out the experimental studies. These 2 metallic nanoparticles were chosen for the study owing to its abundant availability, lower cost and better longevity. Normally 4 methods preferred for preparing nanofluids are namely chemical combustion method, sol-gel method, chemical vapour deposition method

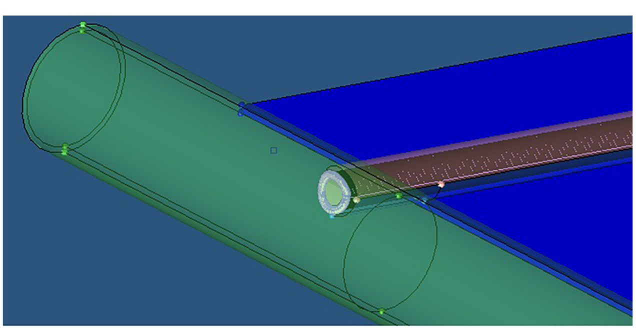

Fig. 14 Internal finned tube CAD

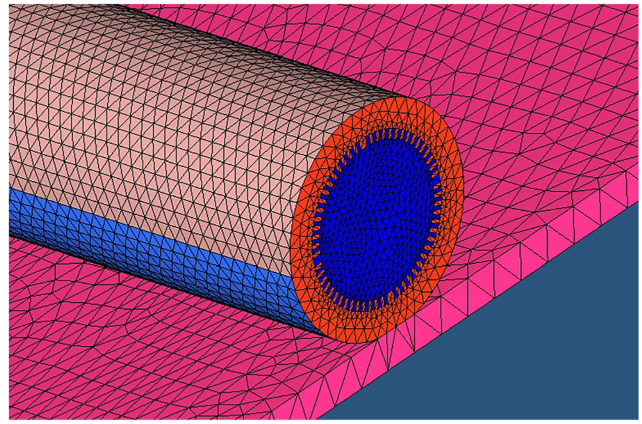

Fig. 15 Internal finned tube-meshed model

and oxide precipitate method. We have adopted a chemical combustion method (Dinesh Babu et al. 2015) as it is comparatively the most economical, has ability to synthesize lower particle size and has better ease of operation coupled with lower gestation period (Simonetti et al. 2020; Sharafeldin et al. 2019; Bhave and Kale 2020). Details of the nanoparticles synthesized are detailed in Table 2. The fuel used, reaction temperature and molar ratio adopted for both the nanoparticles were urea, 500 °C and 1:1 respectively.

Figures 4, 5, 6 and 7 show the SEM image of synthesis and energy-dispersive X-ray analysis (EDAX) of Al_2O_3 and CuO nanoparticles. The resulting nanofluid was subjected to ultrasonic treatment to aid better suspension of particles in the base fluid.

The thermal properties of synthesized nanofluids were measured by using KD2-PRO-thermal analyser and presented in Table 3.

Phase analysis of the synthesized nanoparticles

The phase analysis is done for both nanofluids and preparation of nanoparticle suspension is the first step of applying fluid in heat transfer enhancement. In the present study, the metal oxide nanoparticles were dispersed in distilled water by ultrasonication without using any dispersant or stabilizer to prevent any possible changes of chemical properties of the nanofluids. Ultrasonication is the process of applying sound energy to agitate particles in a sample, for preparing the homogeneous mixture. The process which uses ultrasonic frequencies for about 20–40 kHz is known as ultrasonication or ultrasonication (Gupta et al. 2015; Mercan and Yurddaş 2019;

Table 4 Mesh details for plain tube riser SFPC

Detail	Plain SFPWHS	Internally finned SFPWHS
Elements	1,602,701	3,690,458
Nodes	313,774	976,542

Table 5 CFD solver selection

Description	CFD setting
Fluid domain	Water
Flow type	Incompressible and steady
Solver	3D pressure-based Navier Stokes
Flow equations	Second-order upwind
Turbulence model	Standard k-Ɛ equation
Equations solved	Continuity X-Momentum Y-Momentum Z- Momentum Energy k-Turbulence Ɛ-Turbulence

Shareef et al. 2015). Sonication is commonly used in nanotechnology for evenly dispersing nanoparticles in liquids. The ultrasonicator used to prepare the nanofluids is shown in Fig. 8. The prepared nanoparticles are cooled to ambient condition and mixed in the required weight fraction with distilled water. The resulting solution is termed the nanofluid and then subjected to ultrasonic treatment for better suspension of a particle in the base fluid. Weight concentration which is a mass ratio of the nanoparticles to the base fluid is used to describe the nanoparticle concentration. This current study used a weight concentration of nanofluids ranging from 0.2 to 0.4% wt. The sample of nanofluids is kept for a period of 45 min.

Stability analysis of nanofluids

The nanofluid stability tested conducted for continuously 24 h and it was observed that there were no traces of settling of nanoparticles during the experimentation. The nanoparticles were added with 0.1% of surfactant (CTAB) which further enhances the proper dispersion of nanoparticles with the base fluid (water). Before doping of nanofluids, the nanofluids were stirred for 6–8 h continuously using a magnetic stirrer to ensure proper dispersion. No traces of settling of

Table 6 Input parameters for the working fluid (water)

Parameters	Dimensions
Inlet temperature	300 K
Density	990.9 kg/m^3
Specific heat	4180 J/kg-K
Thermal conductivity	0.6 W/m-K
Viscosity	0.001003 kg/m-s
Thermal expansion coefficient	0.00021 1/K
Mass flow rate	0.0143 kg/s
Velocity	0.0303 m/s

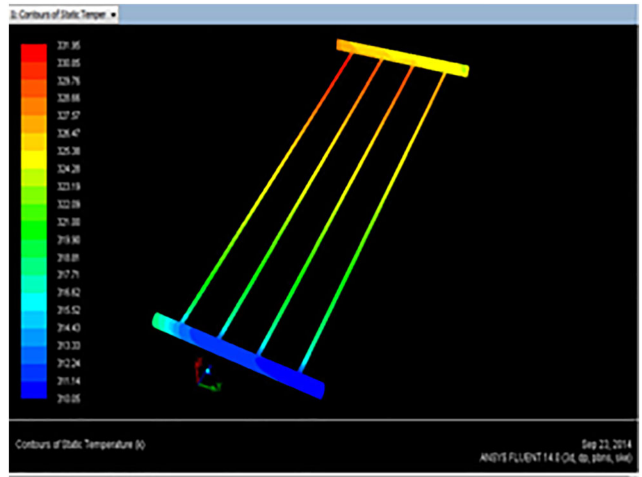

Fig. 16 Temperature distribution for internal finned riser tubes

nanoparticles were observed. A magnetic stirrer has been used for ensuring the uniform dispersion. Figures 9 and 10 show the deployment of a magnetic stirrer to ensure uniform dispersion of Al_2O_3 and CuO nanoparticles.

Irrespective of magnetic stirring, settling was observed when CuO nanoparticles were mixed with water. Hence, dispersants were used to mitigate these settling issues. The addition of dispersants in the two-stage schemes in a straight forward and economical approach improves the steadiness of nanofluids.

Results and discussion

Simulation studies

Simulation is started and the equations are solved iteratively as a steady state or transient. A postprocessor is used for the

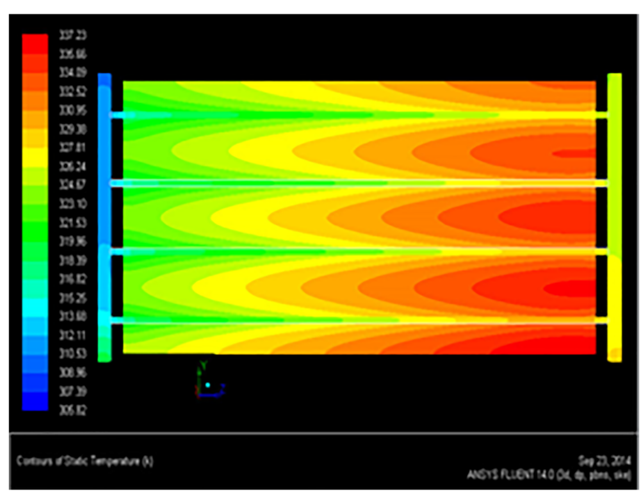

Fig. 17 Temperature distribution along with riser tube plain tube collector

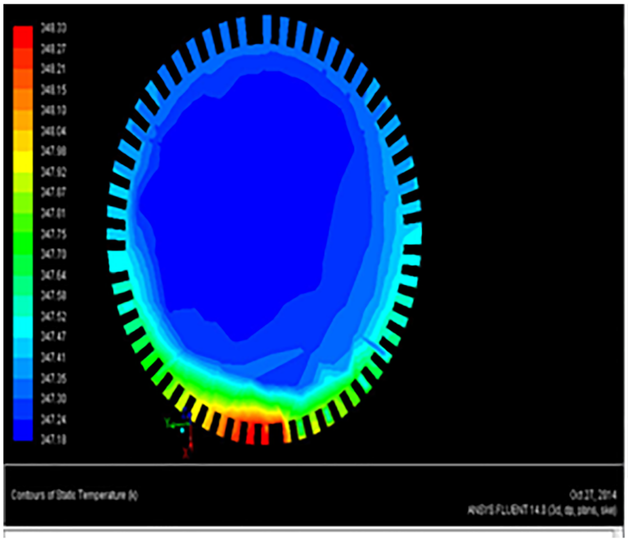

Fig. 18 Temperature variation with internal finned tube collector

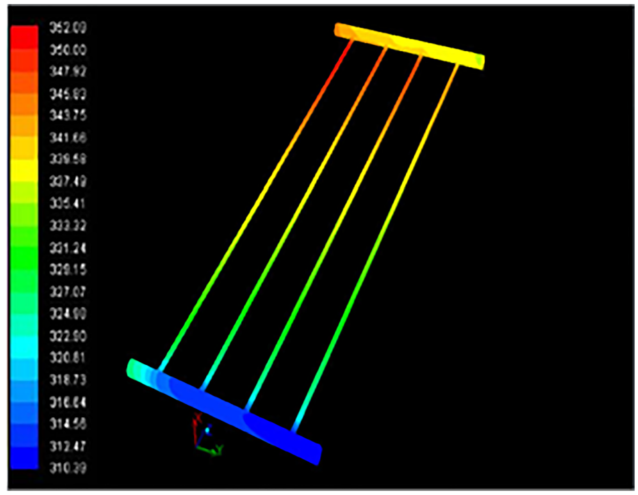

Fig. 20 Temperature variation along with SFPC internal finned tube collector

analysis and visualization of the resulting solution. The following flowchart in Fig. 11 presents the simulation method.

Generating model using Pro-E

The geometrical model of the plain SFPWHS system was created using Pro-E depicted in Figs. 12 and 13. The model (in IGS format) was imported to HyperMesh for meshing.

A similar approach was adopted for the internally finned SFPWHS and the outcome is depicted in Figs. 14 and 15. Mesh details for the plain and internally finned tube riser SFPC are presented in Table 4. The details regarding the CFD solver selection are presented in Table 5.

Numerical solutions are obtained for transient laminar flow with the Boussinesq approximation for modelling of buoyancy to consider a variation of density with a variation of temperature. Table 6 details the values accounted for the working fluid (water).

Solution convergence

The meshed model of solar FPC has imported into ANSYS Fluent 14 for simulation. A constant heat flux equivalent to the solar insolation was applied at the top surface. The bottom and side surfaces of the absorber plate and the outer surface of the absorber tube are defined as the wall with zero heat flux condition (Anbarsooz et al. 2020; Sadeghi et al. 2020; Ma et al. 2019). The simulation defined with 500 iterations and precision of the solution defined up to 10^{-7}. It is observed that the riser which is near to the outlet has more temperature compared with that of other riser tubes inside the collector. The

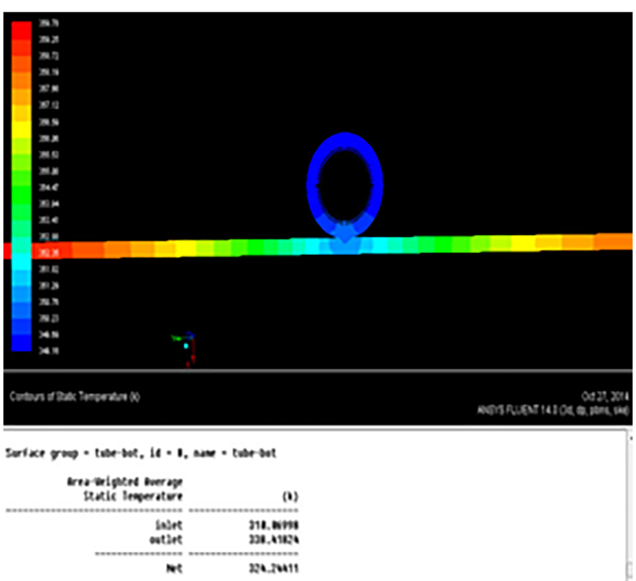

Fig. 19 Temperature variation in finned riser and absorber plate section

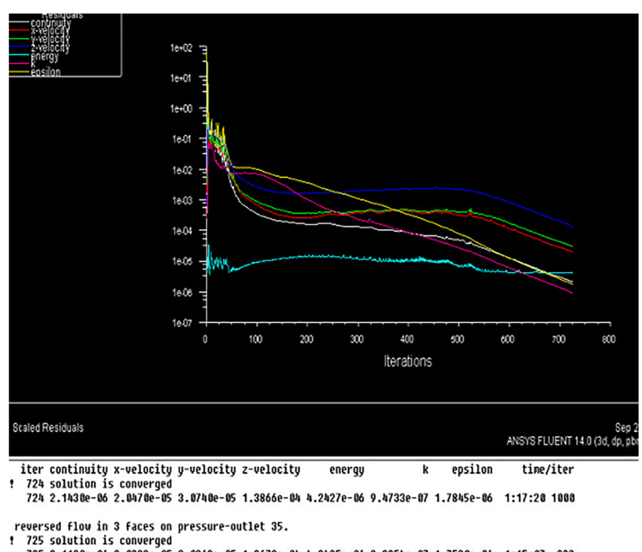

Fig. 21 Convergence diagram of finned riser tubes

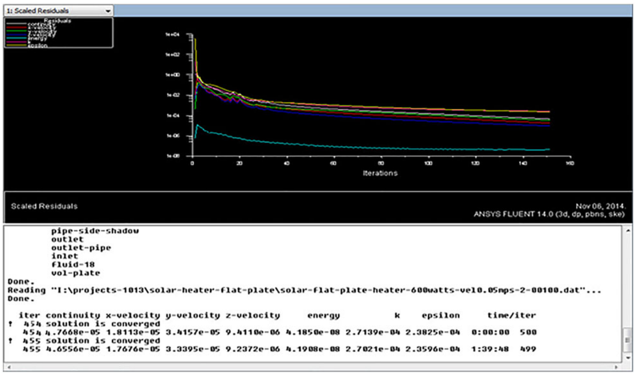

Fig. 22 Convergence diagram of unfinned riser tubes

convergence chart, temperature distributions and variation along the entire solar flat plate collector for the plain tube and for the internally finned riser tubes obtained using CFD analysis are shown in Figs. 16, 17, 18, 19, 20, 21 and 22. It is observed that the riser which is near to the outlet has more temperature rise than the other risers.

Based on the simulation results, it was observed that for the same insolation values and inlet temperature value with and with finned riser tube, SFPC was simulated and outlet temperatures are noted and presented in Table 7. It is apparent that outlet temperature values of SFPC with internal helical fins are higher compare with that of the plain tubes of SFPC by about 5.62 °C.

Uncertainty analysis

The test was conducted for 2 days continuously for each working fluids for both the finned and unfinned tube collectors and the error which occurred during the conduct of an experiment is done using the uncertainty analysis. The inaccuracy is intended for thermocouples and solarimeter. Ambiguity accompanying with the experimental dimensions is shown in Table 8.

Mathematical uncertainty analysis

The result R is a given function of the independent variables $x_1, x_2, \ldots x_n$.

Thus, $R = R\ (x_1, x_2, x_3,, x_n)$.

Let ω_R be the uncertainty in the result and $\omega_1, \omega_2, \ldots, \omega_n$ be the uncertainties in the independent variables. If the uncertainties in the independent variables are all given with the same odds, then the uncertainty in the result having these odds is given as (Beemkumar et al., 2019)

Table 8 Experimental uncertainty errors

Instrument	Accuracy	Range	% Error
Thermocouples	± 0.01 °C	0–200 °C	0.03%
Solarimeter	± 5 W/m^2	0–1000 W/m^2	0.19%

$$\omega_R = \left[\left(\frac{\partial R}{\partial x_1} * \partial x_1\right)^2 + \left(\frac{\partial R}{\partial x_2} * \partial x_2\right)^2 + \ldots + \left(\frac{\partial R}{\partial x_n} * \partial x_n\right)^2\right]^{\frac{1}{2}} \quad (1)$$

If this relation is applied to the energy and exergy efficiency of the previous section,

$$\omega_\eta = \left[\left(\frac{\partial \eta}{\partial I} * \partial I\right)^2 + \left(\frac{\partial \eta}{\partial T_i} * \partial T_i\right)^2 + \left(\frac{\partial \eta}{\partial T_o} * \partial T_o\right)^2\right]^{\frac{1}{2}} \quad (2)$$

$$\omega_\eta = 1.05\%$$

Comparison of outlet temperature for finned and conventional (unfinned) type collectors using different working fluids

The variation of solar insolation with respect to time during the experimental days was measured and was plotted for different working days for different working fluids, shown in Figs. 23 and 24. The readings were taken on a bright sunny day with a clear sky and the air maximum temperature is 33 °C and minimum temperature is 24 °C. The measurements were performed in Chennai, Tamil Nadu, India: latitude 13.66° N; longitude 80.11° E; altitude 58.29° N. As can be inferred, the variation in irradiation values during the period of trial seems to be insignificant.

Both the fabricated solar flat plate water heating systems (one with internal fins and other conventional plain tubes) were made to operate in parallel. Initially, water was used as the working fluid and the efficiency of both the SFPWHS was computed experimentally, by duly considering the insolation and heat absorbed by the SFPWHS. These results were fixed as the baseline. Water was then discharged and alumina nanofluid of 0.2% weight fraction was charged to the system and performance evaluation studies were carried out. Trials were repeated for 0.4% weight fraction of alumina, 0.2% and 0.4% weight fraction of copper oxide nanoparticles. Surfactant CTAB was used for both the nanofluids to ensure better dispersion and suspension of nanoparticles. After

Table 7 Comparison of outlet temperature for with and without finned tube

Inlet water temperature (°C)	Solar insolation (W/m^2)	Simulated outlet temperature no fin (°C)	Simulated outlet temperature with fin (°C)	ΔT (°C)
38.08	783	62.87	68.49	5.62

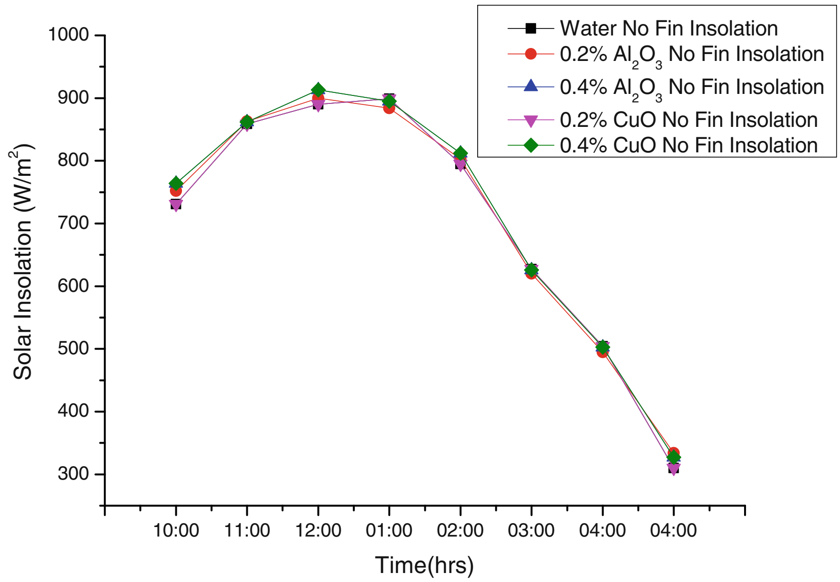

Fig. 23 Solar insolation for no fin tube

baseline fixation with water, the trial is conducted with nanofluids in order to study the heat transfer enhancement for the exit temperatures for both the finned and unfinned tube collectors. During experimentation, it was observed that there was a significant improvement in outlet temperature by doping of nanoparticles in terms of weight fractions. The doping of nanoparticles has better heat transfer enhancement which further increases the outlet temperatures for the collectors, most importantly by minimizing the heat loss and knack of absorbing the heat from the radiation side (solar energy). Both the fin and unfinned tube collectors were subjected to performance trials. Temperature and insolation were taken and adopted for calculating efficiency. Figures 25, 26, 27 and 28 depict the variation of the outlet temperature of different weight fractions of the Al_2O_3 nanofluids.

Evaluation of collector efficiency using different weight fractions of Al_2O_3 and CuO nanofluids and water for with and without riser tubes

Among the different geometrical collectors analysed, it is apparent that outlet temperature values of SFPC with internal helical fins are higher compare with that of conventional type (no fin) collectors because of the presence of the internal helical fins in the SFPC. Efficiency is calculated for the different weight fractions of Al_2O_3 and CuO nanofluids and with base fluid distilled water. The synthesized Al_2O_3 and CuO

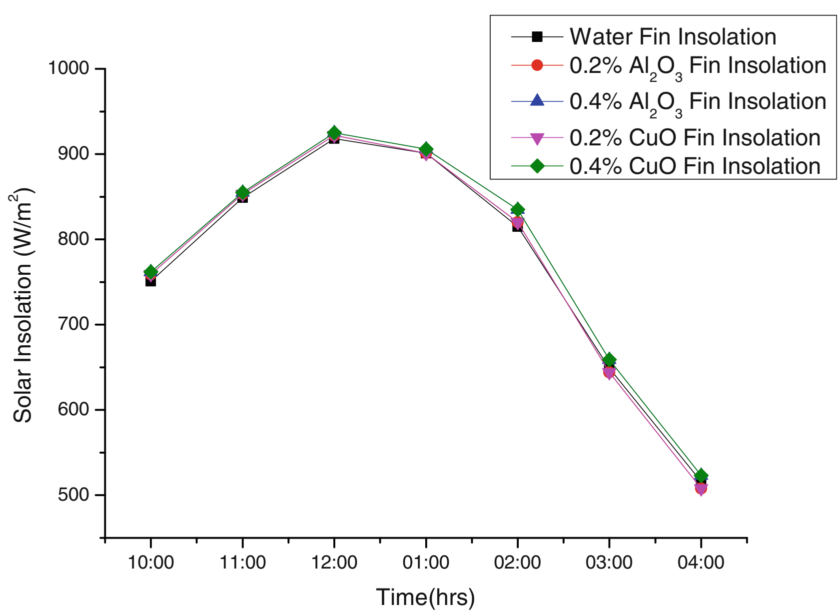

Fig. 24 Solar insolation for fin tube

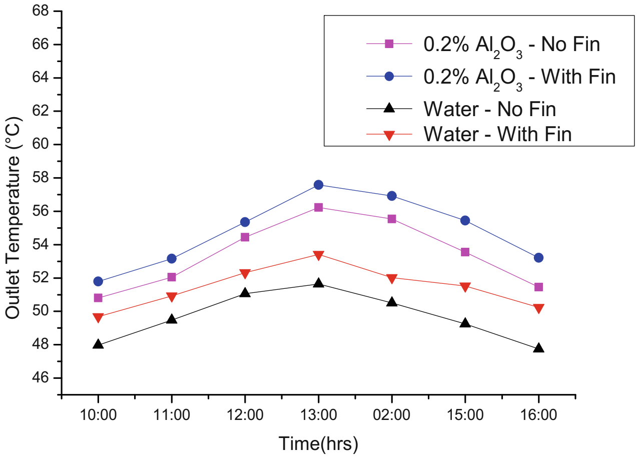

Fig. 25 Comparison of outlet temperatures for 0.2% wt fractions of Al_2O_3 nanoparticles and water

nanoparticles of different weight fractions and water are tested both for internal grooved fin and conventional (no finned) tube collectors. During the conduct of the experiment, the end efficiency compared with that of plain (unfinned) tube subjected to Al_2O_3 and CuO nanofluid outcome showed that the internally grooved-finned tube collectors achieve the maximum and water and the graphs plotted for the efficiency vs. time are shown below in Figs. 29, 30, 31 and 32. The Al_2O_3 and CuO nanofluid is the best option to increase the collector efficiency without much alteration in the existing collector profile and its lifetime also increases, eliminating the corrosion problem completely such as scaling in riser tube which affects the collector performance in due course of time (Guo et al. 2020). It was pragmatic that for a grooved-finned construction, tube collector achieved a high efficiency than conventional (unfinned) tube collector (Zeng and Xuan 2018; Hazra et al. 2019). A renowned "Hottel-Whillier-Bliss" equation was used to determine the efficiency of collectors. The addition of nanoparticles had a significant impact on the temperature of the working fluid. Increasing weight fraction revealed occurrences of higher temperatures which improves a greater thermal efficiency on the collector side. And the experimental consolidated results for internal finned and unfinned riser tube collectors with different working fluids are shown in Fig. 33.

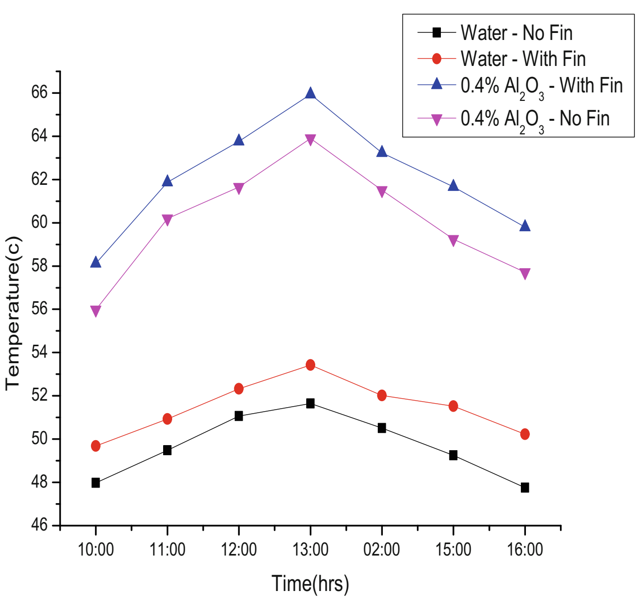

Fig. 26 Comparison of outlet temperatures for 0.4% wt fractions of Al_2O_3 nanoparticles and water

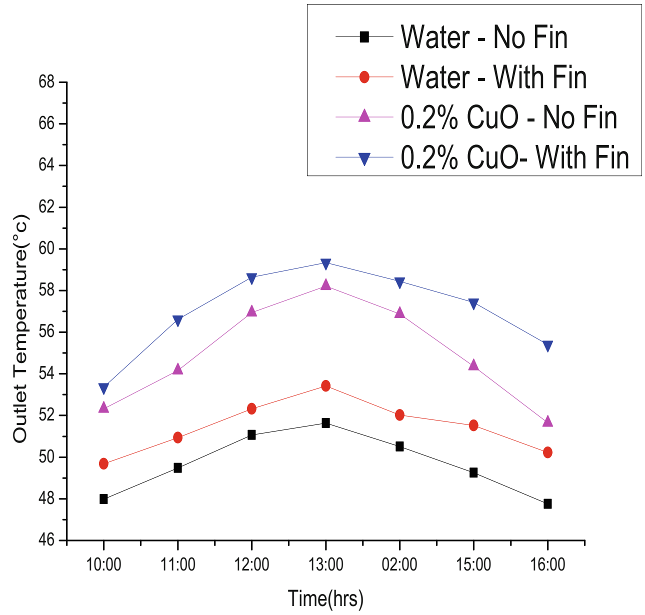

Fig. 27 Comparison of outlet temperatures for 0.2% wt fractions of CuO nanoparticles and water

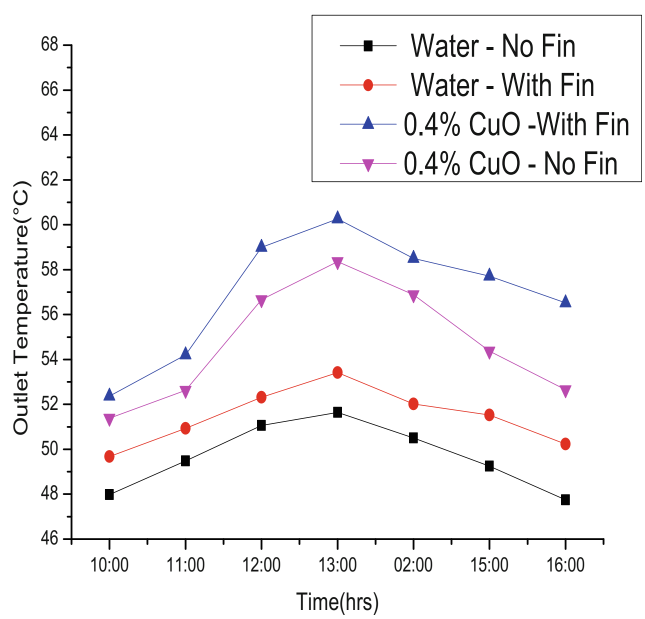

Fig. 28 Comparison of outlet temperatures for 0.4% wt. fractions of CuO nanoparticles and water

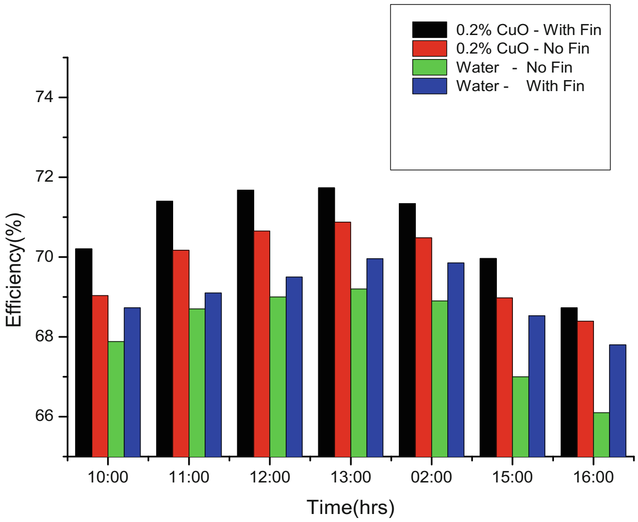

Fig. 29 Comparison of η for 0.2% weight fraction of CuO nanofluid

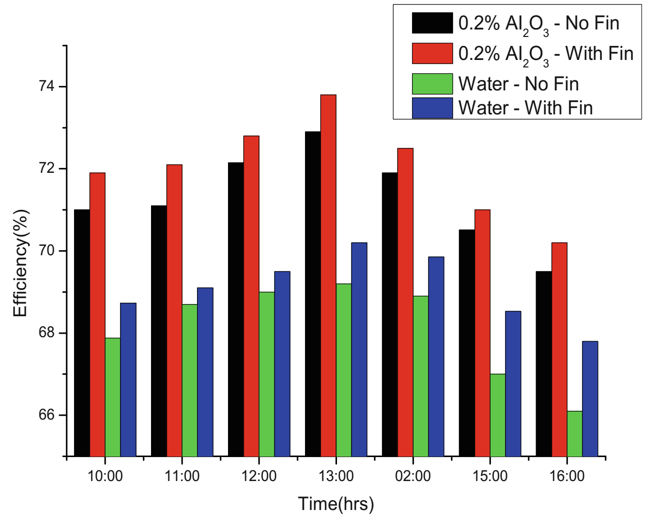

Fig. 31 Comparison of η for 0.2% weight fraction of Al2O3 nanofluid

Conclusion

The main objective of this study is to confront the solar flat plate water heating systems to maximize the efficiency and grab the solar energy from the solar irradiation and change into the valuable transfer of heat energy. The area of the solar collector is used to augment the heat transfer rate where heat is received from the sun. To enhance the efficiency of solar flat plate water heating systems (both finned and unfinned) by the use of nanofluids, it will enhance the heat transfer rate by increasing the thermal conductivity of working fluid. The following conclusions are obtained from the experimental investigations:

1. An experimental investigation on 25-LPD solar flat plate collector system with two different geometries of riser tubes was carried out separately.
2. The thermal performance of solar flat plate collector is enhanced with synthesized nanofluids than the base working fluid (water) for different concentrations.
3. A 25-LPD solar flat collector of internally finned and plain (unfinned) riser tubes was designed for theoretical and experimental observation.
4. Enhancing the thermal conductivity enhanced the rate of heat transfer of nanofluid.
5. The collector efficiency is improved by 4% by employing Al_2O_3 nanofluid for the finned tube. A total of 3% improvement was observed by employing CuO nanoparticles and water.
6. Al_2O_3 nanofluid reaches peak efficiency than CuO nanoparticles and conventional working fluid (water) owing to its enhanced rate of heat transfer. Further, the internal finned tube collector results in higher efficiency than a conventional collector.
7. Based on the simulation results, it was observed that for the same insolation values and inlet temperature value for

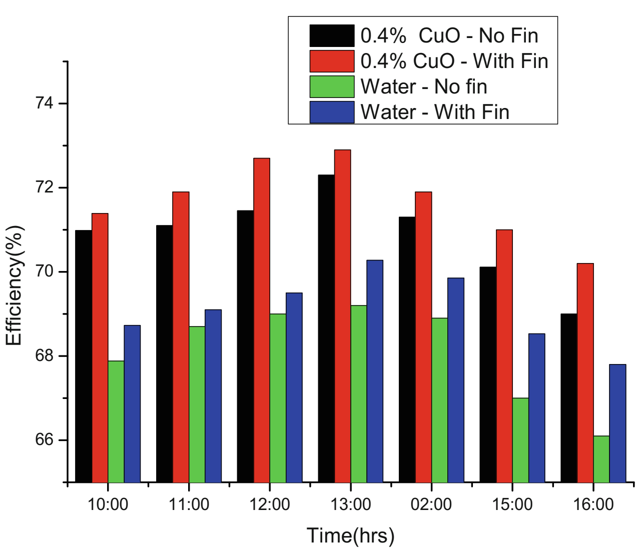

Fig. 30 Comparison of η for 0.4% weight fraction of CuO nanofluid

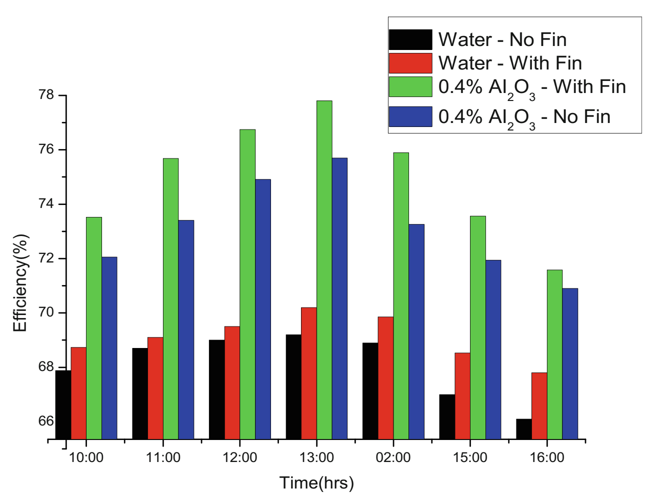

Fig. 32 Comparison of η for 0.4% weight fraction of Al2O3 nanofluid

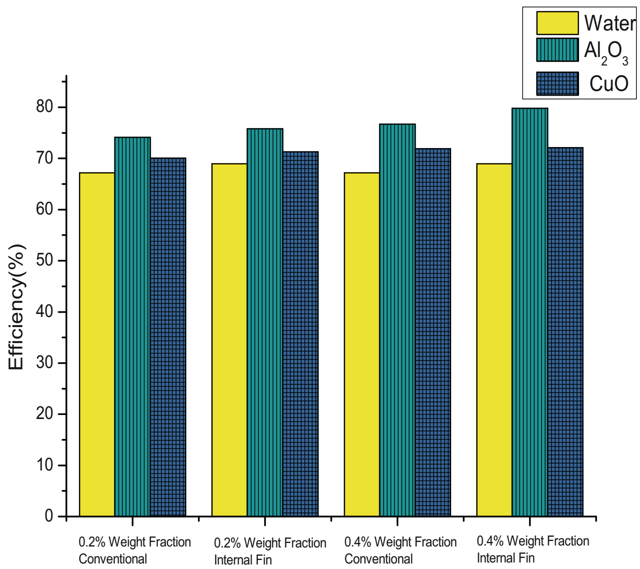

Fig. 33 Comparison of the efficiency of weight fractions of nanofluids in SFPWHS

with and with finned riser tubes, SFPC is simulated and outlet temperatures are noted.

Scope for future work

Further to this study, it is realistic to broaden the area of research in the field of solar energy by employing collectors with varying geometries:

1. Usage of varying nanofluids with different thermal properties can be studied for collector performance,
2. Study and analyse the collector performance using very less viscous domestic oils (kerosene, coconut oil, sea same oil, groundnut oil and sunflower oil) on the heat transfer characteristics.
3. Different nanoparticles can be synthesized for diverse particle sizes and also minimizing the surface area of nanoparticles for ensuring the proper dispersion with base working fluid water in order to study the thermal performance of solar water heating systems.

References

Anbarsooz M, Amiri M, Rashidi I, Javadi M (2020) Heat transfer augmentation in solar collectors using nanofluids: a review. Curr Biochem Eng 06:72–81. https://doi.org/10.2174/2212711906666200225110357

Aparna Z, Michael M, Pabi SK, Ghosh S (2019) Thermal conductivity of aqueous Al_2O_3/Ag hybrid nanofluid at different temperatures and volume concentrations: an experimental investigation and development of new correlation function. Powdertechnology 343:714–722. https://doi.org/10.1016/j.powtec.2018.11.096

Aruna V, Channakaiah, Murali G (2015) A study on a flat plate type of solar water heater with an thermosyphon using different working fluid. Int J Eng Trends Technol 22(10):493–496

Beemkumar N, Yuvarajan D, Arulprakasajothi M, Ganesan S, Elangovan K, Senthilkumar G (2019) Experimental Investigation and Numerical Modeling of Room Temperature Control in Buildings by the Implementation of Phase Change Material in the Roof. Journal of Solar Energy Engineering 142(1). https://doi.org/10.1115/1.4044564

Bhave AG, Kale CK (2020) Development of a thermal storage type solar cooker for high temperature cooking using solar salt. Sol Energy Mater Sol Cells 208:110394. https://doi.org/10.1016/j.solmat.2020.110394

Chatur MG, Nitnaware PT (2015) Experimental investigation on efficiency of flat plate solar collector with BN/H_2O nanofluid. Int J Sci Res Dev(IJSRD) 3(3):2652–2655

Daniels JW, Heymsfield E, Kuss M (2019) Hydronic heated pavement system performance using a solar water heating system with heat pipe evacuated tube solar collectors. Sol Energy 179:343–351. https://doi.org/10.1016/j.solener.2019.01.006

Dinesh Babu M, Venkata Ramanan M (2015) Experimental analysis on the influence of internal finning on the efficiency of a solar flat plate using Al_2O_3 nanoparticles. J Non-Equilibrium Thermodyn 40(3):185–192

Dinesh Babu M, Venkata Ramanan M (2016) Experimental analysis on the performance of a solar flat plate water heater with and without fins. Int J Ambient Energy. https://doi.org/10.1080/01430750.2016.1155496

Dinesh Babu M, Venkata Ramanan M, Mukunthan M (2015) Comparison of the effect of Al_2O_3 and CuO nanoparticles on the performance of a solar flat–plate collector nanoparticles. J Non-Equilibrium Thermodyn 40(4):265–273

Faizal M, Saidur R, Mekhilef S (2013) Potential of size reduction of flat-plate solar collectors when applying MWCNT nanofluid. IOP Conf Series: Earth and Environmental Science. https://doi.org/10.1088/1755-315/16/1/012004

Gangadevi R, Agarwal S, Roy S (2013) A novel hybrid solar system using nanofluid. Int J Eng Res Technol 6(6):747–752

Guo C, Liu C, Jiao S, Wang R, Rao Z (2020) Introducing optical fiber as internal light source into direct absorption solar collector for enhancing photo-thermal conversion performance of MWCNT-H2O nanofluids. Appl Therm Eng 173:115207. https://doi.org/10.1016/j.applthermaleng.2020.115207

Gupta HK, Agrawal GD, Mathur J (2015) Investigations for effect of Al_2O_3–H_2O nano-fluid flow rate on the efficiency of direct absorption solar collector. Case Stud Thermal Eng 5:70–78

Hazra SK, Ghosh S, Nandi TK (2019) Photo-thermal conversion characteristics of carbon black-ethylene glycol nanofluids for applications in direct absorption solar collectors. Appl Therm Eng 163:114402. https://doi.org/10.1016/j.applthermaleng.2019.114402

He Y, Wang S, Ma J, Tian F, Ren Y (2011) Experimental study on the light-heat conversion characteristics of nanofluids. Nanosci Nanotechnol Lett 3:494–496

HuiminLiu WW, Zhao Y, Deang Y (2015) Field study of the performance for a solar water heating sytems with MHPA-FPCS. Energy Procedia 70:79–86

Karmare SV, Tikekar AN (2010) Analysis of fluid flow and heat transfer in a rib grit roughened surface solar air heater using CFD. Sol Energy 8:409–417

Kumar V (2019) Thermal and thermohydraulic performance analysis of three sides artificially roughened solar collectors. Sol Energy 190:212–227. https://doi.org/10.1016/j.solener.2019.08.018

Lu L (2011) Thermal performance of an open thermosyphon using nanofluids for high-temperature evacuated tubular solar collectors (indoor experiment)'. J Solar Energy Eng 85:379–387

Ma T, Ren T, Chen H, Zhu Y, Li S, Ji G (2019) Thermal performance of a solar high temperature thermochemical reactor powered by a solar simulator. Appl Therm Eng 146:881–888. https://doi.org/10.1016/j.applthermaleng.2018.10.025

Manjunath MS, Karanth KV, Yagnesh Sharma N (2012) A comparative CFD study on solar dimple plate collector with flat plate collector to augment the thermal performance. World Acad Sci Eng Technol 70: 969–975

Mercan M, Yurddaş A (2019) Numerical analysis of evacuated tube solar collectors using nanofluids. Sol Energy 191:167–179. https://doi.org/10.1016/j.solener.2019.08.074

Michael JJ, Iniyan S (2015) Performance of copper oxide/water nanofluid in a flat plate solar water heater under natural and forced circulations. Energy Convers Manag 95:160–169. https://doi.org/10.1016/j.enconman.2015.02.017

Munuswamy DB, Yuvarajan D (2016) Analysis on the influence of nanoparticles of alumina, copper oxide, and zirconium oxide on the performance of a flat-plate solar water heater. Energy Fuel 30(11): 9908–9913

Okafor B (2013) Thermosiphon solar water heater. Int J Eng Technol 3(3):312–316

Qu J, Zhang R, Wang Z, Wang Q (2019) Photo-thermal conversion properties of hybrid CuO-MWCNT/H_2O nanofluids for direct solar thermal energy harvest. Appl Therm Eng 147:390–398. https://doi.org/10.1016/j.applthermaleng.2018.10.094

Sadeghi G, Najafzadeh M, Ameri M (2020) Thermal characteristics of evacuated tube solar collectors with coil inside: an experimental study and evolutionary algorithms. Renew Energy 151:575–588. https://doi.org/10.1016/j.renene.2019.11.050

Said Z, Saji MH, Alim MA, Saidur R, Rahim NA (2014) Experimental investigation of the thermophysical properties of Al_2O_3-nanofluid and its effect on a flat plate solar collector. Int Commun Heat Mass Transfer 48:99–107

Sharafeldin MA, Gróf G, Abu-Nada E, Mahian O (2019) Evacuated tube solar collector performance using copper nanofluid: energy and environmental analysis. Appl Therm Eng 162:114205. https://doi.org/10.1016/j.applthermaleng.2019.114205

Shareef AS, Abbod MH, Kadhim SQ (2015) Experimental investigation on a flat plate solar collector using Al_2O_3 nanofluid as a heat transfer agent. Int J Energy Environ 6(4):317–330

Shkhair MM, Sanke N (2015) Heat transfer analysis of a riser tube in a flat plate collector with fins. Int J Mag Eng Technol Manag Res 2: 163–167

Simonetti M, Restagno F, Sani E, Noussan M (2020) Numerical investigation of direct absorption solar collectors (DASC), based on carbon-nanohorn nanofluids, for low temperature applications. Sol Energy 195:166–175. https://doi.org/10.1016/j.solener.2019.11.044

Tiwari AK, Ghosh P, Sarkar J (2013) Solar water heating using nanofluids-a comprehensive overview and environmental impact analysis. Int J Emerg Technol Adv Eng 3(3):221–224

Yousefi T, Veisy F (2012) An experimental investigation on the effect of Al_2O_3-H_2O nanofluid on the efficiency of flat–plate collectors. Renew Energy 39:293–298

Yousefi T, Veisy F, Shojaeizadeh E, Zinadini S (2012) An experimental investigation on the effect of MWCNT-H_2O Nanofluid on the efficiency of flat–plate collectors. Exp Thermal Fluid Sci 39:207–212

Zeng J, Xuan Y (2018) Enhanced solar thermal conversion and thermal conduction of MWCNT-SiO2/Ag binary nanofluids. Appl Energy 212:809–819. https://doi.org/10.1016/j.apenergy.2017.12.083